

# A Novel HE Corrugation Modelling Approach Utilising Conjugate Heat Transfer Methodology

E. Greiciunas \*, Dr D. Borman\* and Dr J. Summers\*  
Corresponding author: scegr@leeds.ac.uk

\* University of Leeds, Woodhouse Lane, Leeds, LS2 9JT, United Kingdom

**Abstract:** An asymmetric serrated Heat Exchanger (HE) corrugation has been evaluated across the Reynolds number range using Computational Fluid Dynamics (CFD) methodology. The corrugation was used in a prototype plate-fin HE unit which was manufactured and experimentally tested. Two detailed computational models for evaluating the HE corrugation are presented: finite length channel and the HE section models. The finite length channel model used a single period width geometry with the setup based on Zheng et al. [1]. A proposed novel HE section corrugation model utilises the conjugate heat transfer methodology. It enabled to study of cross-flow effects between the two HE flow streams providing with the more accurate heat transfer predictions and is previously unseen in the literature. The finite channel flow resistance data is used to verify the results of the HE section domain. The computations were performed using the open-source CFD package OpenFOAM.

*Keywords:* Computational Fluid Dynamics, Heat Transfer, Heat Exchangers, Forced Convection, OpenFOAM.

## 1 Introduction

Heat Exchangers (HE) are devices used in aerospace, automotive and other industries for the energy transfer between the two or more separated fluid streams [2]. The efficiency of the HE is critical for the performance of the overall system of interest stimulating the need for optimised design procedures. Traditional HE modelling methodology, summarised by Kays and London [3] relies on empirical/analytical correlations for the thermal and pressure drop performance estimations. Using CFD simulations for predicting the flow and heat transfer performance of the HE unit is an emerging alternative and is typically accomplished in two steps. Firstly, a small section of the HE core is modelled using detailed CFD analysis to acquire detailed flow and thermal performance data. This data is then used in modelling HE unit which uses flow and heat transfer simplifications inside the HE core [4, 5]. The detailed analysis of the HE corrugation is typically completed in literature by either modelling only a single period of the HE corrugation [6] or by a utilising a finite length channel [1]. However, in both domains the heat transfer mechanisms are limited or require analytical treatment as provided in Kays and London [3] to make the data applicable for a wider range of scenarios. In this paper an industrial serrated plate-fin HE corrugation is firstly simplified using the fully periodic flow assumption [6] to aid efficient modelling of the larger computational domains. The simplified geometry model is then implemented in two main detailed corrugation computational domains. Finite length model which is set up according to Zheng et al. [1] and analyses a single width channel corrugation model across the cold flow layer. A second approach is a novel HE section model utilising the conjugate heat transfer methodology. It allows studying the cross-flow heat transfer effects between the two fluid streams occurring in a lot of compact HE which is impossible using the conventional methodology. The results of the two models are compared in terms of the flow resistance factor to verify the novel HE section model.

## 2 Background and Methodology

A compact plate-fin HE was used in this study with 10 cold and 9 hot layers with identical serrated corrugation in cross flow orientation made using a traditional stacked plate approach. The schematics of the HE core (each layer of  $\approx 80 \times 60 \times 2.5 \text{ mm}$ ) and the corrugation are shown in Figure 1. Aluminium alloy was used for the HE unit with the properties given in Table 2 whilst the properties of aviation fuel and engine oil were used for the cold and hot streams respectively and provided in Table 3. The following governing equations were used for the predictions [7]:

$$\nabla \cdot \mathbf{u} = 0 \quad (1)$$

$$\rho \frac{\partial \mathbf{u}}{\partial t} + \rho(\mathbf{u} \cdot \nabla) \mathbf{u} = -\nabla p + \mu \nabla^2 \mathbf{u} + S \quad (2)$$

$$\frac{\partial T}{\partial t} + \mathbf{u} \cdot \nabla T = \alpha(\nabla^2 T + \Phi) \quad (3)$$

where for the periodic flow cases the source term  $S$  in the flow momentum equation was used as in Patankar et al. [6]. Across the simulations presented in this paper the fluid was assumed to be laminar, incompressible

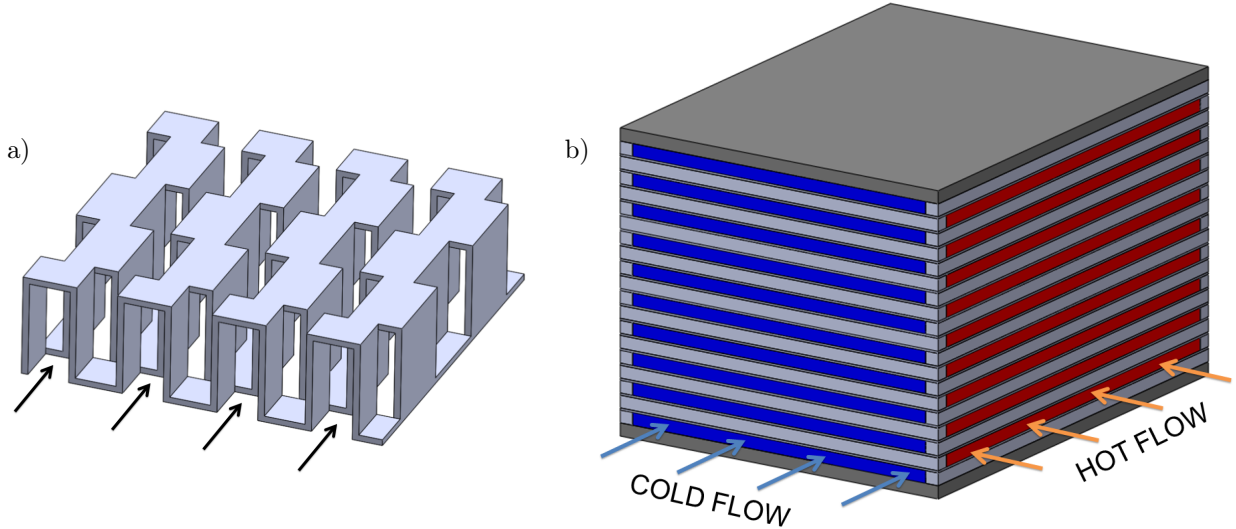


Figure 1: a) Schematic example of the serrated (off-set strip) corrugation and b) HE core model with the flow directions.

and with constant fluid and solid properties. In the majority of cases the predictions were steady state with the computational domains being discretised as in Table 1. Simulations using the transient flow assumption were completed using the first order implicit Euler OpenFOAM scheme. This resulted in using either `buoyantBoussinesqSimpleFoam` or `buoyantBoussinesqPimpleFoam` solvers depending on the case with the buoyancy disabled to comply with the modelling assumptions stated above.

	Discretisation scheme
Gradient	Gauss linear
Pressure	Gauss linear corrected
Momentum	bounded Gauss linearUpwind
Turbulent kinetic energy	bounded Gauss upwind
Specific dissipation rate	bounded Gauss upwind
Energy	bounded Gauss linearUpwind

Table 1: Summary of discretisation schemes used for simulations.

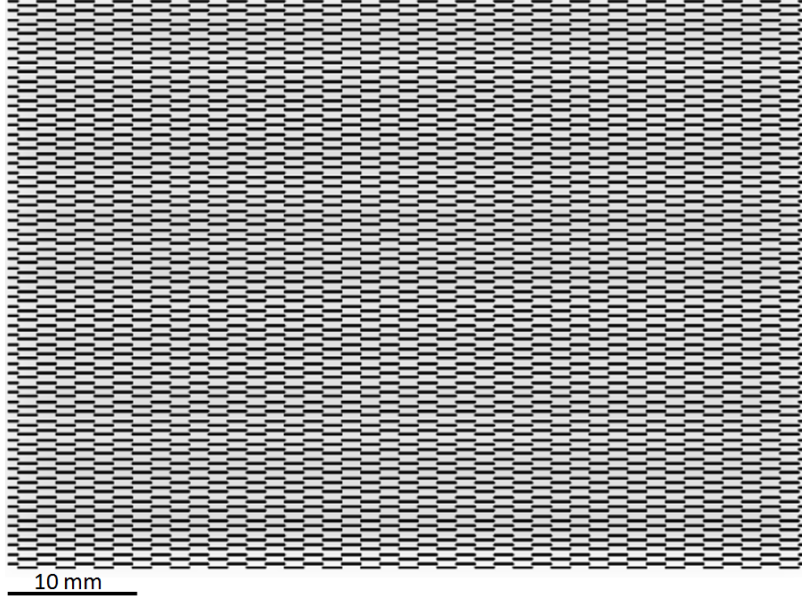


Figure 2: Slice through the cold flow layer of the HE core.

Property	Quantity	Units
Density	2739	$kg/m^3$
Thermal Conductivity	168	$W/(mK)$
Specific Heat	910	$J/(kgK)$

Table 2: Properties of the aluminium alloy used at room conditions.

The meshing process was undertaken using the OpenFOAM inbuilt methodology where a base mesh for the part is established with `blockMesh` application and then refined to the geometry of the part utilising the `snappyHexMesh` application. The afore mentioned need for the various computational domain simplifications arrives from the flow elements present in compact HE and a small hydraulic diameter ( $d_h \approx 1\text{ mm}$ ) in this application. Figure 2 shows the number of flow elements present in only one of the 19 layers clearly illustrating that it is computationally infeasible to study the HE unit using fully detailed three-dimensional CFD. In this case the HE was manufactured with an industrial asymmetric serrated corrugation used in a prototype unit for both fluid sides which also required a bigger computational domain compared to a symmetric serrated geometry often found in the literature (Figure 3).



Figure 3: Cut through of the periodic flow domain showing the asymmetric pattern of the corrugation.

The original geometry of the corrugation was also complex (Figure 4a) and required simplifications for more efficient meshing and computations. Thus, the three simplifications were produced shown in Figures 4b,c and d. All the corrugation domains were analysed using the periodic flow assumption using the global

	Cold flow, $\Delta T$ test	Hot flow, $\Delta T$ test	Cold flow, $\Delta P$ test	Units
$\rho$	781	926	743	$ks/m^3$
$\mu$	0.0012	0.0031	$6.1 \times 10^{-4}$	$Pa \cdot s$
$C_p$	2020	2111	-	$J/(kgK)$
$Pr$	18	50	-	-

Table 3: Cold and hot flow side fluid properties based on the experimental testing.

pressure gradient across the selected Reynolds number range in Figure 5. The meshes for all four domains were produced by **snappyHexMesh** had identical mesh refinement levels and were limited to the cell amount of 80000. Whilst the full mesh independence was not undertaken in this step the meshes were generated by the user to an acceptable resolution based on the experience allowing to ensure similarity of the different solutions.

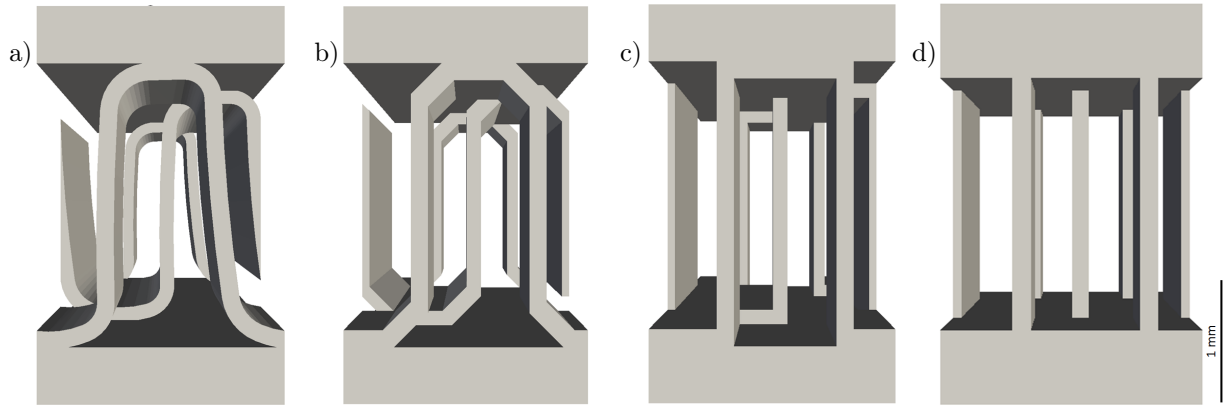


Figure 4: a) Original plate-fin corrugation together with the simplifications of a b) Chamfered, c) Squared and d) Squared2 models.

The periodic predictions below  $Re = 300$  were obtained using the steady state solvers for all the domains. At  $Re = 300$  the steady state simulations started diverging suggesting the requirement of the transient flow solver, a similar finding to the previous study by the author [8]. This suggests that the unsteady flow behaviour in such applications occurs from low flow rates in the HE away from the inlet to the core. The flow instability levels were measured using the errorbars (Figure 5) by using the standard deviation function in Matlab during post-processing of the results. It contrasts with the previous study [8] where flow unsteadiness levels were higher suggesting less significant influence of the fluid mixing to this particular corrugation geometry. Overall, the Figure 5 revealed that only the chamfered simplification of the domain was acceptable (Figure 4b) and did not distort the results in terms of the a global pressure gradient across the domain, a quantity often used in macro scale HE core modelling.

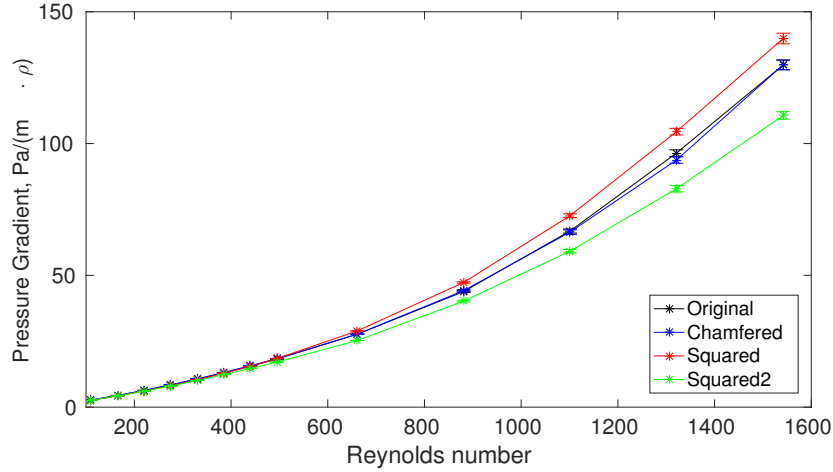


Figure 5: Overall pressure gradient results with errorbars to show fluctuation levels of the flow.

The simplified chamfered corrugation model then allowed to construct the two main detailed corrugation domains of interest. The first domain, is shown in Figure 6 is a finite length single channel of a 50% cold flow layer length. The constant temperature condition was applied to the domain walls following the methodology of Zheng et al. [1] in order to provide with the heat transfer in the flow-wise direction as well as the pressure drop information.

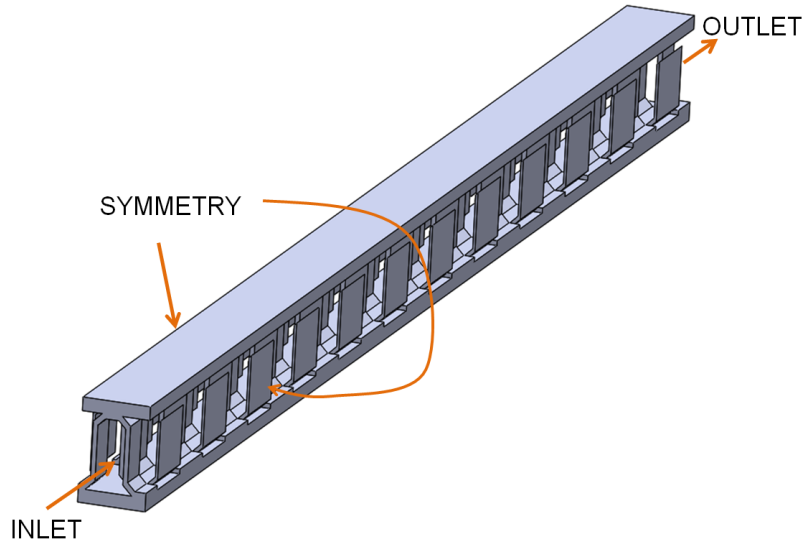


Figure 6: Serrated half length ( $\approx 40 \text{ mm}$ ) of the cold flow side single channel corrugation model with boundary conditions used for meshing.

The second domain is shown in Figure 7 involved the novel HE section model containing both cold and hot flows of the HE. The thermal effects between the two models were connected through the solid corrugation with the conjugate heat transfer solver of OpenFOAM being used to acquire and post-process solutions. For the simulations, the cold domain was split in half to surround the hot flow in order to replicate the conditions of the overall heat transfer unit (10 cold and 9 hot flow layers in the unit).

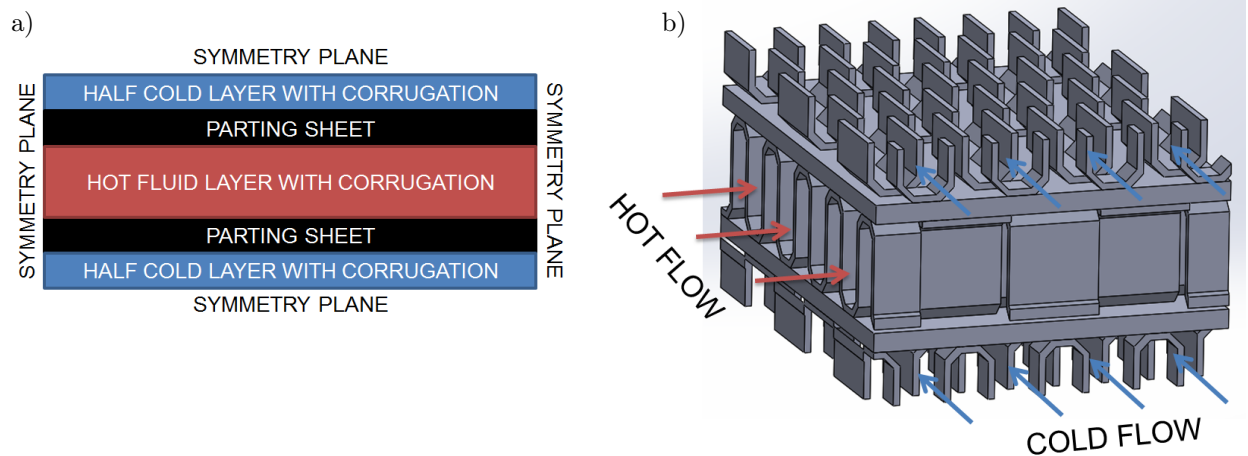


Figure 7: a) Schematic of the conjugate problem b) solid domain visualisation of 1/16th of the layer area.

### 3 Results

Firstly, the mesh independence of the solutions was achieved for both single channel and the HE section computational domains by varying the mesh refinement levels with `snappyHexMesh` application within OpenFOAM. The example outputs of the HE section domain are shown in Figures 8 and 9 clearly presenting the cross-flow thermal effects being captured between the two layers - a result previously impossible with the single corrugation width domains. However, the HE section model was found requiring a mesh of at least 2.5 times the size compared to the single channel domain in order to produce accurate results. The increase of the mesh was particularly high due to the high compactness level of the design leading to a lot of high resolution near wall mesh to be generated. The additional computational intensity of the larger HE section model also meant that the meshes were generated of an overall slightly lower resolution compared to the single channel domain.

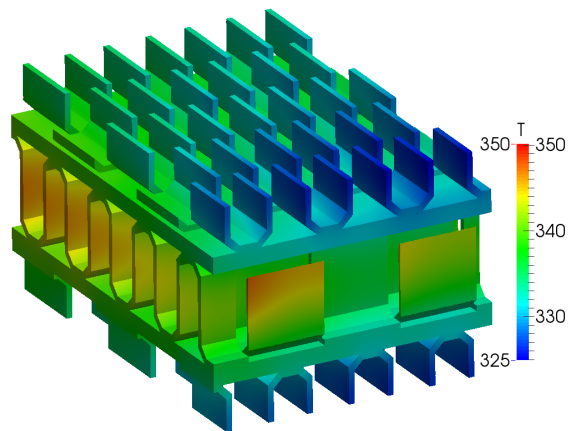


Figure 8: Output of the solid domain at  $Re = 146$  and  $Re = 35$  at the cold and hot side of the HE respectively.

To provide with more information about the two computational domains were also increased in size whilst maintaining the same mesh resolution through `snappyHexMesh` settings. Single channel domain was increased to the full length of the cold flow layer whilst HE section model was increased twice in the cold direction only. The selective increase for the HE section model was undertaken as during the HE unit experiments only the cold flow rate was varied whilst the hot flow remained at a constant flow rate at a low Reynolds number

inside the HE core. This modification allowed maintaining a mesh independent solution whilst lowering the cost of the initial mesh independence calculations.

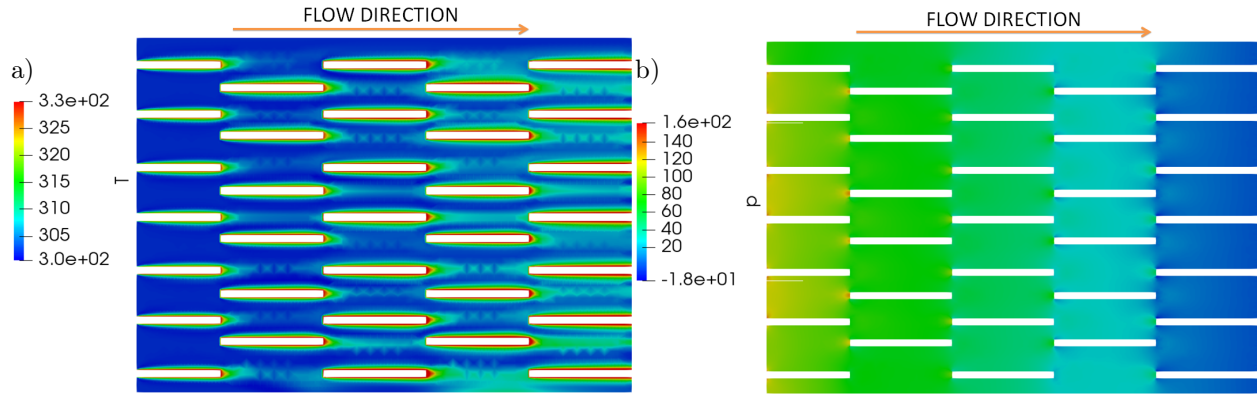


Figure 9: Visualisations at middle of the top flow domain of a) Temperature and b) pressure contours at  $Re = 146$  at medium mesh resolution. Flow direction is from left to right.

In order to check the similarity of the results, f factor from a version of the Forchheimer formulation [9] was used:

$$\nabla p = \frac{1}{2} f \rho \mathbf{u}_f^2 \quad (4)$$

where  $u_f$  - flow velocity magnitude at the inlet to the domain. The periodically developing flow resistance data of the two domains using the cold flow characteristics is shown in Figure 10. The higher resolution of the the single channel model led to overall, slightly higher prediction of the friction factor, especially during the development phase of the flow whilst the middle periods of the two domains agreed quite well. The majority of the heat transfer (Figure 9a) was also found to occur for the both domains during the flow development highlighting the need for flow mixing. The last period friction factor data for the HE section model was thought to be influenced by the flow exit effects. It was decided to omit the results of the last period whilst calculating the average flow resistance across the cold side of the HE corrugation to avoid the artefact.

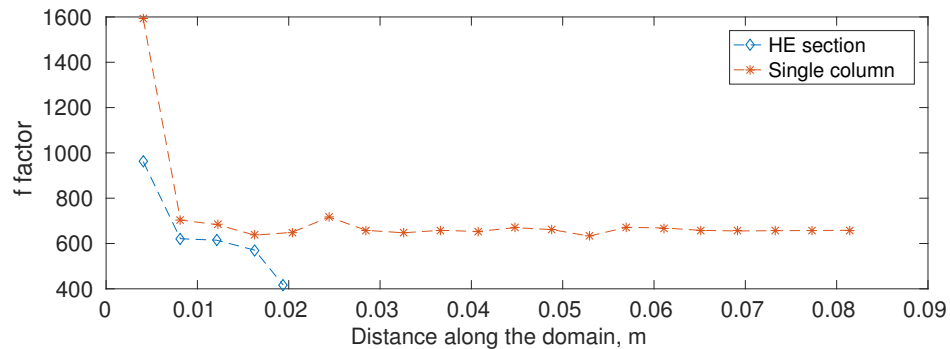


Figure 10: Periodically changing f factor along the cold flow direction comparison between the two simulation domains at  $Re = 146$ .

The average flow resistance characteristics for the cold side of the corrugation were also compared in Figure 11 between the two detailed domains. This quantity would be used in the HE unit modelling rather than having variable resistance making the results in Figure 11 of greater importance. The results clearly show that whilst the periodic development of the flow was found to be slightly different, the averaged

quantities across the operational range agree well. In addition, the results in Figure 11 provides verification of the more complex HE section domain.

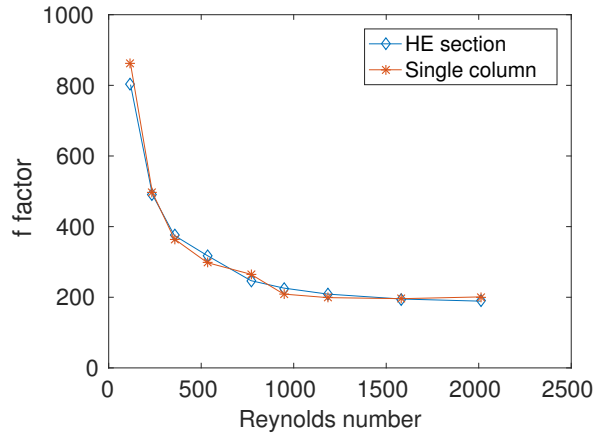


Figure 11: Comparison of the overall f factors across the two detailed corrugation domains.

High quality experimental data was also used to validate the results of the CFD modelling approaches described in this study across the broad Reynolds number range. The data was acquired at the HE unit level and overall a close agreement was found between the experiments and the CFD simulations for both pressure drop and heat transfer performance. However, as the results were acquired in partnership with an industrial partner we are currently awaiting permission to publish them.

## 4 Conclusions

A novel approach to study the plate-fin HE corrugation was proposed utilising a section of the HE core. It models both, hot and cold working fluids connected through the solid via the conjugate heat transfer methodology to account for the impact of the cross-flow heat transfer effects. The approach has been shown to enable more accurate and realistic simulation of the heat transfer inside the HE compared to the existing methods. The novel computational domain was evaluated against the finite length channel corrugation model based on the established methodology in the literature. Overall, a good agreement was found between the two detailed corrugation domains allowing to verify the HE section domain. High resolution experimental data was also acquired at the industrial facility and used to fully validate the numerical modelling.

## References

- [1] Zhanying Zheng, David F Fletcher, and Brian S Haynes. Transient laminar heat transfer simulations in periodic zigzag channels. *International Journal of Heat and Mass Transfer*, 71:758–768, 2014.
- [2] John E Hesselgreaves. *Compact heat exchangers: selection, design and operation*. Gulf Professional Publishing, 2001.
- [3] William Morrow Kays. *Convective heat and mass transfer*. McGraw-Hill, 1966.
- [4] L Sheik Ismail, Ch Ranganayakulu, and Ramesh K Shah. Numerical study of flow patterns of compact plate-fin heat exchangers and generation of design data for offset and wavy fins. *International journal of heat and mass transfer*, 52(17):3972–3983, 2009.
- [5] Andrew M Hayes, Jamil A Khan, Aly H Shaaban, and Ian G Spearing. The thermal modeling of a matrix heat exchanger using a porous medium and the thermal non-equilibrium model. *International Journal of Thermal Sciences*, 47(10):1306–1315, 2008.
- [6] SV Patankar, CH Liu, and EM Sparrow. Fully developed flow and heat transfer in ducts having streamwise-periodic variations of cross-sectional area. *Journal of Heat Transfer*, 99(2):180–186, 1977.

- [7] Subrahmanyam Chandrasekhar. *Hydrodynamic and hydromagnetic stability*. Courier Corporation, 2013.
- [8] Evaldas Greiciunas, Duncan Borman, and Jon Summers. Unsteady flow modelling in plate-fin heat exchanger channels. In *ASME 2017 Summer Heat Transfer Conference*. American Society of Mechanical Engineers, 2017.
- [9] P. FORCHHEIMER. Wasserbewegung durch boden. *Zeitschrift des Vereines deutscher Ingenieure*, (45):1782–1788., 1901.